[11] Moore, C. B., "Vibration-Rotation Energy Transfer," *Journal of Chemical Physics*, Vol. 43, No. 9, Nov. 1965, p. 2979.

[12] Shin, H. K., "Deexcitation of Molecular Vibration on Collisions: Vibration-to-Rotation Energy Transfer in Hydrogen Halides," *Journal of Physical Chemistry*, Vol. 75, No. 8, Aug. 1971, p. 1079.

[12] Shin, H. K., "Vibration-Rotation-Translation Energy Transfer in HF-HF and DF-DF," *Chemical Physics Letters*, Vol. 10, No. 1, July 1971, p. 81; "Erratum", Vol. 11, No. 5, Nov. 1971, p. 628.

[14] Schafer, T. P., Siska, P. E., Parson, J. M., Tully, F. P., Wong, Y. C., and Lee, Y. T., "Crossed Molecular Beam Study of $F + D_2$," *Journal of Chemical Physics*, Vol. 53, No. 8, Oct. 1970, p. 3385.

[15] Parker, J. H. and Pimentel, G. J., "Vibrational Energy Distribution Through Chemical Laser Studies: I. Flourine Atoms Plus Hydrogen or Methane," *Journal of Chemical Physics*, Vol. 51, No. 1, July 1969, p. 91.

[16] Stephens, R. R., and Cool, T. A., "Vibrational Energy Transfer and De-excitation in the HF, DF, HF-$CO_2$, and DF-$CO_2$ Systems," *Journal of Chemical Physics*.

[17] Wilkins, R. L., "Monte Carlo Calculations of Reaction Rates, II. $H + HF(v) = H_2(v') + F$ and $H + FH(v) = HF(v') + H$," *Journal of Chemical Physics*.

[18] Mercer, P. D. and Pritchard, H. Q., "The Gas Phase Fluorination of Hydrogen Methane Mixtures," *Journal of Physical Chemistry*, Vol. 63, No. 9, Sept. 1959, p. 1468.

[19] Rapp, D. and Englander-Golden, P., "Resonant and Near-Resonant Vibrational-Vibrational Energy Transfer Between Molecules in Collisions," *Journal of Chemical Physics*, Vol. 40, No. 2, Jan. 1964, p. 573.

[20] Rapp, D., "Interchange of Vibrational Energy Between Molecules in Collisions," *Journal of Chemical Physics*, Vol. 43, No. 1, July 1965, p. 316.

[21] Rapp, D. and Kassal, T., "Theory of Vibrational Energy Transfer Between Simple Molecules in Nonreactive Colliisions," *Chemical Reviews*, Vol. 69, No. 1, Feb. 1969, p. 61.

[22] Bott, J. F. and Cohen, N., "Shock Tube Studies of HF Vibrational Relaxation," *Journal of Chemical Physics*, Vol. 55, No. 8, Oct. 1971, p. 3698.

[23] Airey, J. R. and Fried, S. F., "Vibrational Relaxation of Hydrogen Fluoride," *Chemical Physics Letters*, Vol. 8, No. 1, Jan. 1971, p. 23.

[24] deVries, A. E. and Klein, F. S., "Ultraviolet-Induced Isotope Exchanges in Gaseous Mixtures of HCl and $D_2$ and of DCl and $H_2$," *Journal of Chemical Physics*, Vol. 41, No. 11, Dec. 1964, p. 3428.

[25] Ridley, B. A. and Smith, I. W., "The Vibrational Relaxation of HCl ($v = 3$, 2, and 1) by Cl Atoms," *Chemical Physics Letters*, Vol. 9, No. 5, June 1971, 0. 457.

OCTOBER 1972 AIAA JOURNAL VOL. 10 , NO. 10

# Propellant Combustion Instability as Measured by Combustion Recoil

C. M. MIHLFEITH*
*Thiokol/Wasatch Chemical Corporation, Brigham City, Utah*
AND
A. D. BAER† AND N. W. RYAN†
*University of Utah, Salt Lake City, Utah*

**The response function relating mass flux perturbations of a burning solid propellant to externally imposed periodic thermal radiation has been measured over a range of frequencies for several composite propellants. Strands of propellant were mounted on a sensitive, quartz force transducer, and the transient force signal, the combustion recoil, was obtained while exposing the surface to the periodic radiation. Definite maximum in the response was noted at dimensionless frequencies, $\alpha\omega/r^2$, of 20 to 80, depending on the fuel binder, oxidizer loading and propellant translucence. Variations in composition and oxidizer loading produced significant changes in the response which are attributed to the changes in the interfacial combustion dynamics. The total character of the response function was altered by changes of the propellant fuel binder. Lower maximum response at resonance was noted for the PBAA fueled propellants as compared to the polyurethane fueled opaque propellants. The comparison of the characteristics of the measured response functions to predictions of current theoretical models, which were modified to consider radiant heat flux effects for translucent propellant rather than pressure perturbations, suggests general agreement between theory and experiment. The technique is suggested as a laboratory method of studying the influence of propellant formulation variation on solid-propellant combustion dynamics.**

## Nomenclature‡

$C$ = mean heat capacity; $C$ is of propellant, $C_p$ is of gas phase
$C_1$ = $C_p\bar{T}_s/2C_4$
$C_2$ = $E_f\bar{T}_s/2R\bar{T}_f^2 - C_1$
$C_3$ = $E_s/R\bar{T}_s^2C$
$C_4$ = $Q_f - C_p(\bar{T}_f - \bar{T}_s)$
$C_5$ = $C_p/C/E_s/RT_s - C_2 - C_1)/C_2 - C_3C_4$
$E$ = activation energy; $E_s$ of surface pyrolysis, $E_f$ of gas phase reactions
$F$ = heat flux, $F_r$ is radiant flux
$f$ = force transmitted from burning strand to the transducer
$K$ = a proportionality constant in Eq. (6)
$k$ = thermal conductivity; $k$ is of propellant, $k_g$ is of gas phase
$m$ = mass flux from burning surface; $m_f$ is in gas phase; normally, $m = m_f$
$M_f$ = molecular weight of combustion products
$n$ = the pressure exponent for steady-state linear burning rate
$P, p$ = pressure
$Q_f$ = energy released in the flame per unit mass of propellant burned
$R$ = gas constant
$R_f$ = real part of the response function; for the pressure driven case $R_f = (m'/p')(\bar{p}/\bar{m})$, for the flux driven case $R_f = (m'/F_r')(\bar{F}_r/\bar{m})$
$r$ = linear burning rate of the propellant
$T$ = temperature; $T_s$ is the surface, $T_{-\infty}$ is at a distance into the propellant, $T_f$ is the flame temperature, $T_o$ is the temperature at $x = 0$
$t$ = time
$x$ = distance, $x_s$ is of the surface from $x = 0$
$\alpha$ = propellant thermal diffusivity
$\gamma$ = solid opacity, $cm^{-1}$

Presented as Paper 71-209 at the AIAA 9th Aerospace Sciences Meeting, New York, January 25-27, 1971; submitted August 2, 1971; revision received May 15, 1972. This work was supported by the Air Force Office of Scientific Research (AFSC) under Grant 69 AF 69-1656.

Index category: Combustion Stability, Ignition, and Detonation.

* Associate scientist.

† Professor of Chemical Engineering. Associate Fellow AIAA.

‡ A prime (′) denotes the perturbed value of a variable and an overbar (¯) indicates a steady-state or zero frequency value.

$\kappa$ = dimensionless opacity, $\gamma\alpha/\bar{r}$
$\Omega$ = dimensionless frequency, $\alpha\omega/r^2$
$\rho$ = the propellant density
$\omega$ = angular frequency
$\lambda$ = $\frac{1}{2}[1 + (1 + 4i\Omega)^{1/2}]$

## Introduction

SINCE the seriousness of the problem of combustion instability in solid propellant rocket motors was first fully appreciated in the late 1940's, significant effort has been directed toward acquiring a detailed understanding of the phenomenon. Much information has been obtained from unsuccessful motor firings, and more precise knowledge has come from the use of test devices which were designed to exaggerate the instability effects. Theoretical contributions to the state of knowledge in this area have been unusually significant. Nevertheless, a description of this phenomenon which is really adequate for design purposes does not exist. The complexity of the processes by which a burning solid propellant amplifies pressure waves has defied complete analytical description or adequate experimental characterization. The efforts continue; but at the present time, it appears to the authors that significant contributions to knowledge are unlikely to be developed from the now conventional test devices such as $T$-burners and $L^*$-burners. New experimental approaches are required, and the recognition of this need to study combustion instability by use of new techniques which would generate more detailed mechanistic information than the usual phenomenological test motivated the work described here.

Underlying most theories of propellant combustion response to a transient stimulus is the premise that the mass flux-pressure response functions are the most appropriate interface between experiment or design (growth constants) and theory (combustion model). Tests of theories by experiment have been only adequate to give circumstantial support for this premise since mass flux perturbations could only be inferred from measured pressure variations. It is the intent of the work reported here to focus experiment on a coupling function closely related to the mass flux-pressure response function, and thus in some degree to investigate its legitimacy and to define its nature.

All combustion models assume that perturbations in the pressure perturb the feedback heat flux to the burning surface, and by this mechanism (as moderated by the coupled thermal wave in the solid) perturb the mass burning rate. This consideration suggests that another response function, relating mass flux to feedback energy, could be studied with some expectation of defining more precisely the nature of a valid combustion model. Periodic and steady-state radiant heat fluxes were imposed on the surface of burning strands of propellant and the changes in regression rates were evaluated from measurement of the force resulting from combustion-generated momentum. A unique feature of this work is the nearly direct measurement of the mass flux perturbations by use of the "combustion recoil."

## Theory

### Measurement of Burning-Rate Perturbations

The determination of the mass flux from a burning surface as a consequence of a heat flux fluctuation was the major interest in this study. A method used for the determination of the transient mass flux required was to measure the change in force generated normal to the surface when the burning rate of a propellant was modified by an external thermal energy source. By means of a simple momentum balance the total recoil force created by the mass efflux from the burning surface can be developed and is given as

$$f(t) = m(t)^2(RT_f/PM) \tag{1}$$

which for the case of small perturbations can be modified to give the result

$$f'(t) = 2\bar{m}m'(RT_f/PM) \tag{2}$$

Thus, the measured small force perturbations are proportional to variations in the mass burning rate. The experimental problem is to measure these small forces, which can be shown to be on the order of 100 to 300 dyne/cm$^2$.

### Heat-Flux-Burning-Rate Response Function

Theories for the response of the solid-propellant combustion to pressure disturbances have been presented by several investigators[1–8] but the response to thermal radiation has only been briefly treated.[9] The following discussion closely follows the approach employed in most theories for pressure-coupled response; however, in the present case the pressure is treated as constant and a periodic radiant heat flux is assumed to impinge on the burning surface.

### Solid Phase Analysis

The analysis for the opaque solid is essentially identical to the analysis for the solid subjected to a conductive heat flux, the detailed relationships can be found in several places; for example, see Ref. 3 and 10. For the case of the radiatively heated translucent solid, temperature fluctuations are the direct result of radiative flux perturbations and the indirect result of the conductive flux changes produced by mass flux variations. The heat flux variations, $F_r'$, appear as an energy generation term in the perturbed form of the differential equation. Since the energy equation is linear, it is permissible and convenient to express the solid temperature fluctuations as the sun of the radiation contribution, $T_r'$, and the conductive contribution $T_c'$, or $T' = T_r' + T_c'$. The perturbed form of the one-dimensional heat conduction equation containing the convective term is solved for the solid extending from $x = -\infty$ to 0 (at the mean position of the burning surface) for the assumed periodic temperature fluctuations as a result of the periodic radiant heat flux. The variation in the conductive heat flux at the burning surface is obtained and a correction is applied for periodic variation of the surface position about the $x = 0$ position. The heat flux at the surface is given as

$$k(\partial T'/\partial x)_{s-} = \bar{m}C\lambda T_s' + [C(\bar{T}_s - T_{-\infty})/\lambda]m' - m\lambda CT_{or}' \tag{3}$$

This result is used in the energy balance across the gas-solid interface,

$$-k(dT'/dx)_{s-} = [-k_g(dT'/dx)_{s+}] + m'q_s \tag{4}$$

which provides a matching condition for analyses of the two phases. The radiant heat flux $F_r'$ does not appear in Eq. (4) and gradients of $T_r'$ are zero for the translucent solid at the surface.

### Gas Phase Model

The treatment of the gas phase varies the most among various authors studying combustion instability. Although it is generally believed that the flame zone is turbulent and heterogeneous, a result from laminar flame theory for premixed gases is generally used in the analysis of the gas phase. One important feature of these results is that the principal variables which govern the gas phase response are retained, i.e., flame temperature, surface temperature and burning velocity. Here again the analysis follows the work of others, e.g. Ref. 10, closely. The solution to the steady-state thermal energy equation for the gas phase yields an expression for the heat transfer from the gas phase to the propellant surface,

$$k_g(dT/dx)_{s+} = m[Q_f - C_P(T_f - T_s)] \tag{5}$$

The burning velocity in the gas phase can be deduced from the analysis of the combustion zone near the propellant surface. Depending on the form of the assumed model of reaction in the gas phase, sharp flame front or some type of distributed combustion, slightly different expressions for the burning velocity are obtained. For the sharp flame front model, Culick[2] obtains,

$$m = KP^{v_1}T_f^{v_2}\left[1 - \frac{C_p(T_f - T_s)}{Q_f}\right]^{1/2} e^{-E_f/2RT_f} \tag{6}$$

For purposes of this study, $v_1$ is taken as being equal to zero because the pressure is constant and uniform to second-order

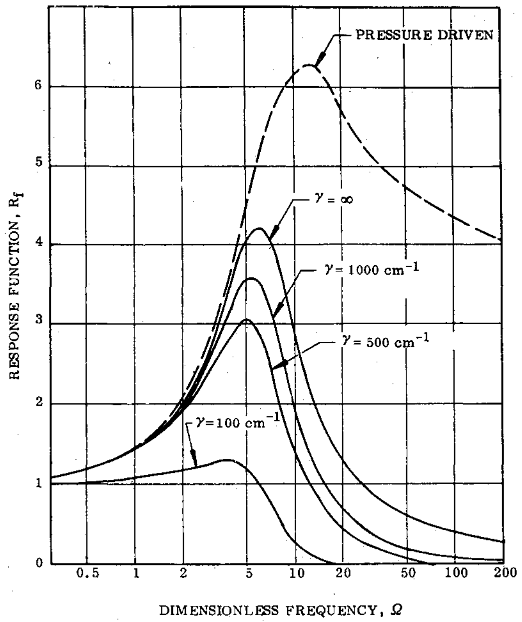


**Fig. 1 A comparison of the real part of the response functions for the pressure and heat flux-driven oscillations of a burning propellant. The same parameters were used in each case.**

perturbations. The parameter $v_2$ is taken as zero[10] since negligible flame temperature fluctuations are expected in this experiment. The final useful result from the above treatment is the perturbed heat transfer to the surface from the gas side and the perturbed burning velocity. The energy equation becomes

$$[k_g(dT'/dx)]_{s+} = m_f'[Q_f - C_p(\bar{T}_f - \bar{T}_s)] - \bar{m}C_p(T_f' - T_s') \quad (7)$$

Perturbation of Eq. (6) yields a relationship between $m'$ and $T_f'$ and $T_s'$. A more sophisticated analysis of the gas phase was not warranted for the interpretation of the experimental data. The assumption of quasi-state behavior within the gas phase was considered to be appropriate for the experimental conditions.

### Burning Rate Response of a Translucent Propellant

The burning rate response to a disturbance in the thermal radiant energy flux was obtained by combination of the several relations described previously

$$\frac{m'}{F_r'} = \frac{C_3((\kappa - \lambda)k/[\kappa^2 - \kappa - \lambda(\lambda - 1)])}{\lambda + A/\lambda + AH + C_5} \quad (8)$$

where $A = (E_s/RT_s)\ [(T_s - T_{-\infty})/T_s]$ is dimensional activation energy and $H = q_s/C(T_s - T_{-\infty})$ is dimensionless surface heat effect.

In the limit as the opacity approaches infinity, this result reduces to that of the opaque propellant case. The real part of Eq. (8) was computed for a range of parameters similar to those used in the case of pressure-driven oscillatory burning. Figure 1 shows a comparison of the computed real part of the response functions for the pressure-driven case, based upon the simple propellant model as for the heat flux-driven case of an opaque propellant and for several values of the opacity. The pressure-driven response function relationships analogous to Eq. (8), contain terms which account for the effect of pressure variations on the gaseous reaction rates and thus the feedback flux.[10] A consistent set of propellant parameters was used. [$\bar{T}_s = 850°K$, $q_s = -25$ cal/g, $E_s/R = 10{,}000°K$, $Q_f = 800$ cal/g, $\bar{r} = 0.2$ cm/sec, $C = 0.33$ cal/(g)(°K), $E_f/R = 25{,}000°K$ and $T_f = 2500°K$.] Each curve was normalized to be asymptotic to a response function of unity at low frequencies.

Although even for the case of the opaque propellant the normalized response functions are not the same as for the pressure-driven case, the same type of qualitative behavior is predicted; and the flux-driven response curves appear to be distinct enough to permit parameter characterization and thus prediction of the pressure response. Since a composite propellant opacity on the order of 500 cm$^{-1}$ would be near to the highest practically obtainable value, a strong effect of energy absorption in depth is predicted; and, in fact, nearly transparent formulations were found to be insensitive to high-frequency flux perturbations.

The response of the burning rate is predicted to lead the flux input at low frequencies, to be nearly zero at the maximum in the response function, and to lag the flux input at high frequencies. Increased transparency of the propellant would result in a tendency for an increase phase lag at all frequencies.

### Experimental Apparatus

Figure 2 shows an over-all schematic of the experimental system. The radiant source was a 5.0 kw xenon-mercury arc lamp at the primary focus of a 21-in.-diam elliptical mirror. The propellant samples were positioned at the secondary focus of the mirror. An 8.5-in.-diam, two-leaf shutter operated by an air piston was used to control the total exposure interval. A 24-in.-diam "chopper" wheel with six segments cut out along the periphery to give equal "open and closed" exposure periods was used to generate a periodic heat flux. This chopper wheel was driven by a dc motor, and the period of exposure was measured by a time interval meter which was triggered by a photo diode. Frequencies from 2 to 300 Hz were used.

The samples were mounted in a combustion chamber which was a 6-in.-diam, 18-in. aluminum cylinder closed at the end opposite to the arc-lamp by a cover plate. All tests reported here were at atmospheric pressure, and the end of the chamber nearest the energy source was open to the atmosphere. Windows placed around the cylindrical walls of the chamber permitted viewing the sample from either side and from above. The entire chamber was mounted on adjustable stages to facilitate three-axis positioning of test areas at the secondary focus of the elliptical mirror.

A three-dimensional map of the secondary focal volume of the image furnace was generated by use of the transient, rate-of-rise calorimeters of the type described by Beyer, McCulley and Evans[11] in which a small hole in a metal disc was used to define the area of measurement. A cylindrical region in which the maximum flux variation was less than 10% existed for 2.5 cm in the axial direction and was 0.6 cm in diameter. The size of this region of essentially constant heat flux was more than adequate for tests with the 0.6 cm diameter strands of 1.0 cm length. The maximum flux from the arc image furnace, which was 14.8 cal/cm$^2$ sec, was attenuated by use of calibrated screens.

The increase in steady-state burning rates produced by the external radiation was measured by means of motion pictures. A 16 mm movie camera with external lenses was focused on the center of the cylindrically-shaped samples and operated at 20 frames/sec during an ignition, a steady nonradiated, and an externally radiated burning sequence. A small scale was mounted with the sample to determine the magnification. The sample length as a function of time was determined from the photographs for each run. These data were used to determine the linear

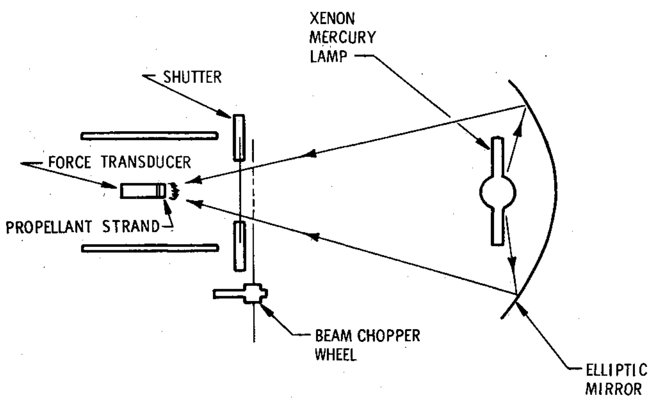


**Fig. 2 The overall experimental system.**

**Table 1 Propellants used for dynamic response experiments**

| Material code | Oxidizer Ammonium Perchlorate | | Fuel/ binder | | Additives | Burning rate cm/sec |
|---|---|---|---|---|---|---|
| UAX | 80% | 40/40[a] | 18% | PU[b] | 2% nbf[c] | 0.20 |
| UCX | 80% | 40/40 | 17% | PU | 2% nbf carbon black, 1% | 0.14 |
| UAY | 80% | 40/40 | 19% | PU | 1% nbf | 0.14 |
| UCV | 80% | 40/40 | 18% | PBAA[d] | 2% CuO2O2P[e] | 0.32 |
| UCW | 80% | 40/40 | 19% | PBAA | 1% carbnn black | 0.15 |
| UAO | 10% | 100% 5μ | 28% | PBAA | 2% CuO2O2P[e] | 0.31 |
| UAQ | 72% | 100% 5μ | 28% | PBAA | | 0.18 |

[a] 50% coarse, +48–100; 50% fine, 5μ or less.
[b] Polyurethane, B.F. Goodrich, Estane based.
[c] N-butyl ferrocene catalyst.
[d] Polybutadiene-acrylic acid copolymer plus 15% Epon 828.
[e] Harshaw Chemical Company catalyst.

burning rate during the test sequence. One advantage of the photographic technique was the visual record of the burning. Anomalous behavior, particularly nonuniform regression, could be recognized and the data from such a test rejected.

The technique devised for transient burning rate measurements employed a Kistler Instrument Model 717 sound pressure microphone. Force was transmitted to the microphone from the burning propellant through a steel rod. The propellant mounting system shown in Fig. 3 eliminated all but the normal force created by the recoil of the burning propellant. The microphone, which responded from 2 to 50,000 Hz, was only sensitive to transient forces. Transient tests showed that the total system response was uniform to 1000 Hz.

The assembly shown in Fig. 3 was placed inside the combustion chamber. A photodiode, RCA 1P42, was placed directly above the transducer, and the photodiode signal indicated the period of sample exposure of the perturbing flux.

The test data were recorded at 65 ips on an instrument tape recorder and were subsequently processed after playback at $4\frac{3}{4}$ ips by measuring the root-mean-square value of the transducer output. A Hewlett-Packard 3400 rms voltmeter was used to determine the average signal level. The dc output from the voltmeter was recorded on a Honeywell 1000 strip chart recorder for detailed examination. The rms signal levels before and after exposure of the sample surface were nearly identical and these signals were subtracted from the radiatively-driven sample signal. The background noise generated by the chopper wheel approached the intensity of the radiatively-driven signal at high frequency and limited the useful upper frequency to about 250 Hz.

The phase angle between the transducer signal and the photodiode signal was measured from the tape records with an AD-YU model 405 phasemeter coupled to the strip chart recorder for direct analog output.

## Experimental Results

Table 1 gives compositions of the various propellants discussed here. Figure 4 summarizes the results of the tests with four propellants in which the atmospheric burning rate was increased by the external flux. The increase was from 5% to 10% of the nonradiated value. The actual heat flux reaching the propellant surface was less than the incident flux as a result of attenuation in the flame. This attenuation was measured by noting the decrease in intensity through capillary tubes inserted through the axis of the strand and through semitransparent samples as the strand ignited. Both methods gave equivalent results; 30–80% of the incident energy was absorbed by the flames. Table 2 summarizes the results on the flame attenuation.

The energy required to gasify the solid at the burning surface $q_s$ can be estimated from the results in Fig. 4 and the flux attenuation data. Table 2 presents such values calculated from the equation,

$$q_s = \frac{1}{\rho(dr/dF)} - C(\bar{T}_s - \bar{T}_{-\infty}) \tag{9}$$

which can be developed from energy conservation arguments, a result required for most instability theories.[1,4,6,7,10–15] These $q_s$ values (negative for exothermic reactions) are subject to the validity of assumed values of the surface temperature and propellant properties. These approximate results are presented here only to indicate that they are of the same magnitude as values assumed in the theoretical calculations.

## Response Function Values

The results from the burning-rate-response experiments indicate clearly that the kind of fuel is an important factor. The data from the polyurethane-fueled propellants lead to a response

**Table 2 Summary of radiation augmented burning studies**

| Propellant | UAO | UAQ | UAX | UAY |
|---|---|---|---|---|
| Fractional radiation loss through flame | 0.5-0.6 | 0.25-0.35 | 0.15-0.25 | 0.15-0.25 |
| Flux sensitivity, $\partial r/\partial Fr$ cm³/cal | 0.0060 | 0.0036 | 0.0037 | 0.0033 |
| Net heat of gasification,[a] $q_s$/cal/g | −65 | ~0 | ~0 | +20 |

[a] Constant values of $I_\infty = 300$ °K, $I_s = 850$ °K, and $pC = 0.55$ cal/(cm³) (°K) were assumed.

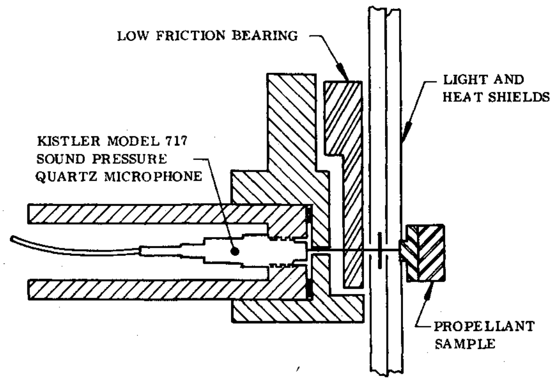


**Fig. 3 The technique used for mounting the propellant sample and transmitting thrust to the force transducer.**

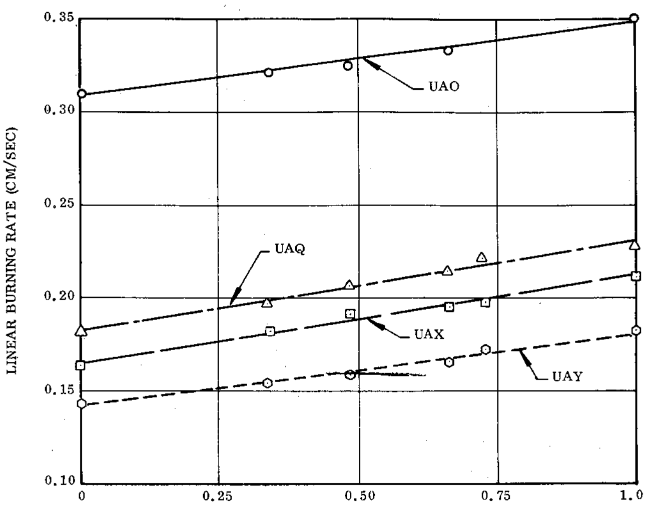


**Fig. 4 The change in linear burning rate at atmospheric pressure produced by a maximum external radiant heat flux of 15 cal/(sec)(cm$^2$). (Table 1 gives the detailed compositions of these propellants.)**

function exhibiting distinct maximum, while those from the PBAA-fueled propellants give a response function showing only a slight maximum. From the results for the polyurethane propellants the effects of the oxidant particle size, the presence of catalyst and the oxidizer-to-fuel ratio were obtained. Two similar PBAA-fueled propellants were studied, and one contained a copper chromite burning rate catalyst.

*PU-AP propellants*

Figure 5 shows the principal features of the propellant response curves for the polyurethane propellants. A linear increase occurs at low frequency, a maximum is observed at a dimensionless frequency of 10–40 (the actual frequencies were from 20 to 80 Hz), and at higher driving frequencies the response rapidly decreases to zero.

Although response functions of five polyurethane propellants were determined, only two are presented here. The UAX and UCX propellants were identical except for an amount of finely dispersed carbon black which replaced some of the binder in the UCX formulation. The radiation absorption coefficient, opacity, of the UAX propellant was less than 100 cm$^{-1}$ whereas that of the UCX propellant was likely about 500 cm$^{-1}$. The comparison in Fig. 5 shows that the translucent propellant exhibited the lesser maximum response and the maximum occurs at a lower frequency.

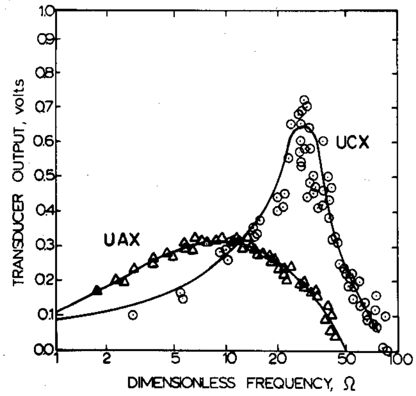


**Fig. 5 The response of the semitransparent polyurethane fueled UAX propellant and the opaque polyurethane fueled UCX propellant to periodic heat flux variation as a function of the dimensionless flux frequency.**

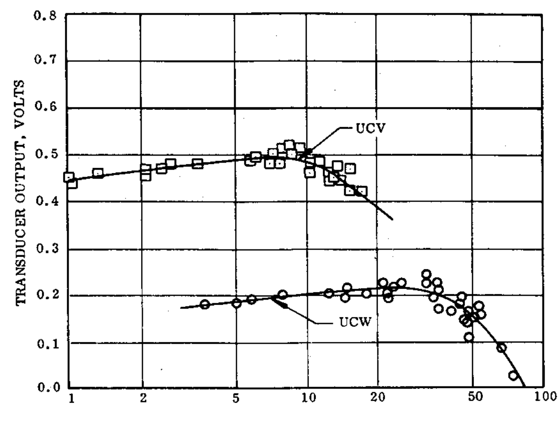


**Fig. 6 The responses of the PBAA-fueled UCW and UCV propellants to periodic heat flux variation as a function of the dimensionless flux frequency.**

*PBAA-AP propellants*

Two PBAA-fueled propellants were prepared and tested in the same manner as the PU-AP propellants. Figure 6 shows data for the UCV and UCW propellant. The low frequency response signal was about the same as for the polyurethane propellants but only a slight maximum in the response was noted at a dimensionless frequency of about 40. The actual frequency of the maximum was 80–90 Hz. Since the burning rate of the PBAA propellants was greater than that for the polyurethane propellants it was not possible to extend the data to high dimensionless frequencies without encountering excessive system-generated noise.

In the case of the PBAA-AP propellants, the uncatalyzed propellant UCW exhibited a response maximum at a higher dimensionless frequency than did the catalyzed UCV propellant. The opposite was noted for the PU-AP system.

*Phase measurements*

Figure 7 shows the measured phase shift between the burning rate perturbations and the heat flux variations for the propellants of interest here as a function of the frequency. In all cases, zero phase difference was measured at low frequencies; however, this was apparently a result of the low frequency limit on the phasemeter. Presumably a phase lead actually occurred. Normally the extrapolated zero phase shift frequency corresponded to the nearly maximum in the magnitude of the response function in agreement with the theoretical predictions.

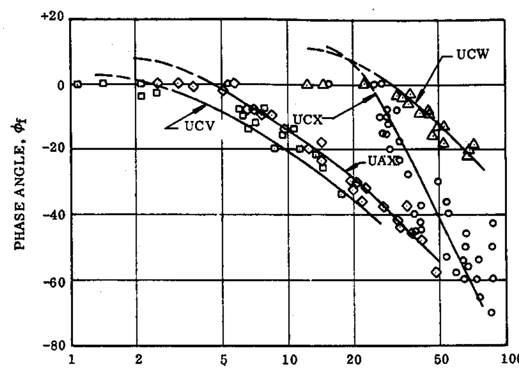


**Fig. 7 The lag angle between the periodic radiation flux as measured by the force transducer as a function of frequency.**

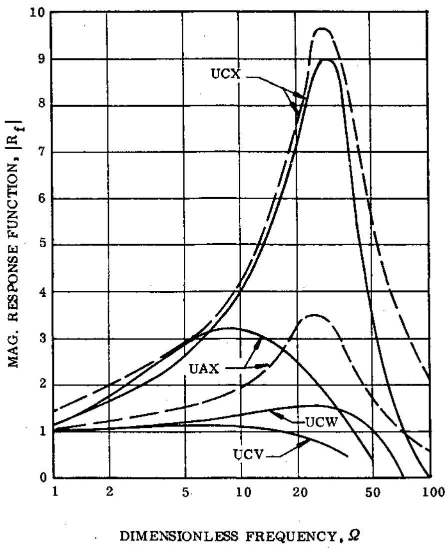


**Fig. 8 A comparison between the magnitude of the response functions calculated from the modified conventional theory and experimental values. The dash lines are for the calculated values.**

## Conclusions

The coupling between feedback energy and the propellant thermal wave long described by theory does, in fact, exist. Gross features of the predicted characteristics of the mass-efflux, heat-flux response functions have been experimentally observed. Quantitative agreement between calculation and experiment can be obtained, although the values of the required theoretical parameters to produce agreement may not be totally realistic. A comparison is presented in Fig. 8 between the predictions of the flux driven combustion model and the data from the polyurethane fueled UAX and UCX propellants. The PBAA based UCV and UCW propellant results are also shown for comparison. This figure is a plot of the magnitude of the response function, which was the experimentally measured quantity, vs the dimensionless frequency with all lines normalized to unity at zero frequency. The experimental values at zero frequency were obtained by extrapolation.

Because the complete response function was generated over a wide range of frequencies, it is possible to establish the parameters which best describe the data, and, in principle, to characterize the propellant.

The parameters selected to approximate the UCX data (the same as for Fig. 1 except $E_s/R = 45{,}000°K$, $\bar{q}_s = -15$ cal/g, $\lambda = 500\ cm^{-1}$, and $\bar{r} = 0.137$ cm/sec) are possibly not a unique set, and these results are presented only to illustrate that agreement between experiment and theory can be obtained. The calculated and measured response phase angles are in quantitative agreement which lends some support to the selected values of the parameters. If the combustion model is correct and the data properly interpreted, it should be possible to satisfactorily predict the pressure driven response or the response under other conditions.

A partial test of this approach is illustrated by comparison of the results obtained from the chemically similar opaque UCX and translucent UAX propellants. In the case of the UAX propellant, the same combustion parameters were used in the calculations but the opacity was reduced to $100/cm^{-1}$. Although the height of the maximum response function was approximately predicted, the shift in the maximum to a lower frequency was not predicted, and no variation in the model parameters produces a significant change in the position of the response maximum when only the transmissivity was changed. This result suggests only a limited predictive capacity of this type of model. Perhaps condensed phase energy effects, which were not considered in the calculations, are important for the semitransparent propellant.

Figure 8 also illustrates the observation that the propellant formulation changes produce significant variations in the response of the burning propellant to the heat flux perturbations. The reproducibility and precision of measurement was great enough to permit observation of differences in response of small changes in composition for a given fuel binder. However, the over-all characteristics of the response were altered drastically by large compositional variations such as by change of fuel binder. Apparently, the polymeric fuel influences the combustion process in a manner not described by considering it to be only a source of gaseous reactants. The UCW data could be described by the combustion model by use of greatly different parameters than those used to compare to the UCV data. Either reducing the magnitude of $E_s$ or changing $\bar{q}_s$ to a large positive value could produce predictions of the type of behavior observed.[16]

The experimental technique of using an energy input to perturb the burning rate developed in this work could be employed as a supplementary method to existing techniques for propellant evaluation. Where directly applicable, considerably more accurate and useful results can be obtained than by any other method. Unfortunately, at present, only tests at atmospheric pressure and on clean burning propellants are possible. Obviously, the next requirement is to eliminate these restrictions, and it is anticipated that such an extension of this technique will be made.

## References

[1] Brown, R. S., Muzzy, R. J., and Steinle, M. E., "Effect of Surface Reactions on Acoustic Response of Solid Propellants," *AIAA Journal*, Vol. 5, No. 9, Sept. 1967, p. 1718.

[2] Culick, F. E. C. and Dehority, G. L., "An Elementary Calculation for the Burning Rate of Composite Solid Propellants," *Combustion Science and Technology*, Vol. 1, July 1969, pp. 193–204.

[3] Culick, F. E. C. and Price, E. W., "Solid Propellant Combustion Instability Studies," NWC Rept. TP 4668, Dec. 1969, Naval Weapons Center, China Lake, Calif.

[4] Denison, M. R. and Baum, E., "A Simplified Model of Unstable Burning in Solid Propellants," *ARS Journal*, Vol. 31, No. 8, Aug. 1961, pp. 1112–1122.

[5] Marxman, G. A. and Wooldridge, C. E., "Effects of Surface Reactions on the Solid Propellant Response Function," *AIAA Journal*, Vol. 6, No. 3, March 1968, pp. 471-478.

[6] Culick, F. E. C., "Calculations of the Admittance Function for a Burning Surface," *Astronautica Acta*, Vol. 13, 1967, pp. 221–237.

[7] Hart, R. W. and McClure, F. T., "Combustion Instability: Acoustic Interaction with a Burning Propellant Surface," *Journal of Chemical Physics*, Vol. 30, Sept. 1959, pp. 1501–1514.

[8] Culick, F. E. C., "A Review of Calculations for Unsteady Burning of a Solid Propellant," *AIAA Journal*, Vol. 6, No. 12, Dec. 1968, pp. 2241–2255.

[9] Cantrell, R. H., McClure, F. T., and Hart, R. W., "Effects of Thermal Radiation on the Acoustic Response of Solid Propellants," *AIAA Journal*, Vol. 3, No. 3, March 1965, pp. 418–426.

[10] Price, E. W. and Culick, F. E. C., "Combustion of Solid Rocket Propellants," *1969 AIAA Professional Study Series.*

[11] Beyer, R. B., McCulley, L., and Evans, M. W., "Measurement of Energy Flux Density Distribution in the Focus of an Arc Image Furnace," *Applied Optics*, Vol. 3, No. 6, June 1964, pp. 131–135.

[12] Krier, H., T'ien, J. S., Sirignano, W. A., and Summerfield, M., "Nonsteady Burning Phenomenon of Solid Propellants: Theory and Experiment," *AIAA Journal*, Vol. 6, No. 2, Feb. 1968, pp. 278–285.

[13] Culick, F. E. C., "An Elementary Calculation of the Combustion of Solid Propellants," *Astronautica Acta*, Vol. 14, 1969, pp. 171–181.

[14] Eisel, J. L., Horton, M. D., Price, E. W., and Rice, D. W., "Preferred Frequency Oscillatory Combustion of Solid Propellants," *AIAA Journal*, Vol. 2, No. 6, June 1964, pp. 1319–1323.

[15] Yang, J. Y. S., "Some Problems in Solid Propellant Combustion Instability," Ph. D. thesis, 1970, Dept. of Mechanical Engineering, Univ. of Utah, Salt Lake City, Utah.

[16] Mihlfeith, C. M., Baer, A. D., and Ryan, N. W., "The Response of a Burning Solid Propellant Surface to Thermal Radiation," AFOSR Scientific Rept. TR-71-2664, AD 736049, Aug. 1971, Univ. of Utah, Salt Lake City, Utah.